

## Simple horizontal magnetic tweezers for micromanipulation of single DNA molecules and DNA–protein complexes

Christopher P. McAndrew<sup>1,2,†</sup>, Christopher Tyson<sup>2,5</sup>, Joseph Zischkau<sup>3,††</sup>, Patrick Mehl<sup>2</sup>, Pamela L. Tuma<sup>4</sup>, Ian L. Pegg<sup>1,2</sup>, and Abhijit Sarkar<sup>1,2</sup>

<sup>1</sup>Department of Physics, The Catholic University of America, Washington, DC, <sup>2</sup>Vitreous State Laboratory, Washington, DC, <sup>3</sup>Carnegie Mellon University, Pittsburgh, PA, <sup>4</sup>Department of Biology, The Catholic University of America, Washington, DC, and <sup>5</sup>Department of Biomedical Engineering, The Catholic University of America, Washington, DC

†Current address: U.S. Patents and Trademarks Office, Alexandria, VA 22314

††Current address: YinzCam, Inc., 5541 Walnut St., Pittsburgh, PA 15232

*BioTechniques* 60:21-27 (January 2016) doi 10.2144/000114369

Keywords: single molecule–micromanipulation; magnetic tweezers; differential measurement; magnetic trap

Supplementary material for this article is available at [www.BioTechniques.com/article/114369](http://www.BioTechniques.com/article/114369).

We report the development of a simple-to-implement magnetic force transducer that can apply a wide range of piconewton (pN) scale forces on single DNA molecules and DNA–protein complexes in the horizontal plane. The resulting low-noise force–extension data enable very high-resolution detection of changes in the DNA tether's extension: ~0.05 pN in force and <10 nm change in extension. We have also verified that we can manipulate DNA in near equilibrium conditions through the wide range of forces by ramping the force from low to high and back again, and observing minimal hysteresis in the molecule's force response. Using a calibration technique based on Stokes' drag law, we have confirmed our force measurements from DNA force–extension experiments obtained using the fluctuation–dissipation theorem applied to transverse fluctuations of the magnetic microsphere. We present data on the force–distance characteristics of a DNA molecule complexed with histones. The results illustrate how the tweezers can be used to study DNA binding proteins at the single molecule level.

Magnetic tweezers have emerged as a powerful tool for studying DNA–protein interactions at the single molecule level (1–8). They are well-suited for experiments applying controlled forces on macromolecular tethers while monitoring their extensions (the latter are subject to thermal fluctuations and, thus, measured extensions are thermally averaged). Tethers have superparamagnetic particles attached to one end that are subject to forces in the 0.1 piconewton (pN) to 100 nanonewton (nN) range when placed in non-uniform magnetic fields (sufficient to saturate the particles) (3,9,10). The magnetic fields are produced using permanent magnets or

electromagnets (11,12). The twist of DNA can also be manipulated by rotating the magnets (2). Recent designs allow simultaneous and independent application of forces and torques (13,14), and one report (15) describes a way to decouple twist fluctuations from applied forces. Other developments include a portable version (16), a design with sub-nanometer extension precision (17), a magnetic system for steering beads (18,19), integration of a very high speed camera (20), magnetic micromanipulation of confined DNA (21), and use of proteins (instead of DNA) as tethers (22).

DNA in magnetic tweezers is typically attached to one end of a microscope

coverslip, with the other end connected to a 1- $\mu$ m scale superparamagnetic particle (1). Above the sample cell is a magnet system for force generation leading to pulling forces in the vertical plane. This design is sometimes referred to as vertical magnetic tweezers. Its strengths include simplicity, the ability to control DNA topology with minimal modifications, and the relative ease with which tethered DNA can be located. It is also the most commonly used variant, which facilitates inter-lab data reproducibility studies. However, in its simplest configuration, the drawbacks of the vertical magnetic tweezers set-up include the requirement to re-acquire

### METHOD SUMMARY

We describe horizontal magnetic tweezers capable of high-precision extension measurements on DNA molecules attached to two beads. The resulting differential extension measurement leads to passive drift compensation and low noise extension measurements.

tethered magnetic beads as they move in and out of the focal plane with changes in extension and susceptibility to sample cell drift. Modifications have been made to generate large forces (3,10), and near-Brownian-limit extension measurements are possible by counting the diffraction rings from beads (3,23,24). Feedback-based active compensation of sample chamber drift has also been implemented (6,25) and is required for long-duration (~1 h) measurements. However, these improvements lead to considerable design complexity.

Another possibility is to apply tension on tethers in a horizontal orientation (25–29). This simplifies extension measurements since calibration between vertical displacement and diffraction ring counts is not required. Moreover, when used with DNA tethers with non-magnetic beads on one end and superparamagnetic beads on the other, extensions can be obtained by a differential measurement technique allowing passive drift cancellation, a feature thus far exploited mainly for optical tweezers (30). Indeed, Yan et al. (26) developed such a scheme using a combination of micropipette aspiration on the non-magnetic bead and a permanent bar magnet to apply magnetic forces on the superparamagnetic bead. However, their open cell design led to increased buffer evaporation and coupling to noise sources. Horizontal tweezers based on single-bead tethers (with direct attachment of the other end of the tether to a glass coverslip) have also been reported (25,27–29). Here, a major concern is determining the position of the tether attachment point or of a fiducial mark on the coverslip. A number of calibration schemes are used, for example, fringe counting, (27) or the overstretching transition (25). However, these procedures are sensitive to stage drift, requiring stage stabilization methods (6,25) that increase system complexity.

Here we report the development of simple-to-implement yet versatile horizontal magnetic tweezers using linear DNA tethers connected to 2 beads that can be built for \$50,000. (Supplementary Table S1 provides a comprehensive list of components, vendors, model numbers, and prices.) While our instrument is a refinement of the ideas presented in Reference 26, we go beyond that work by (i) incorporating a sample cell with a single, narrow open slit that minimizes buffer evaporation and coupling to pressure fluctuations at the open interface; (ii) by using a second micromanipulator to indepen-

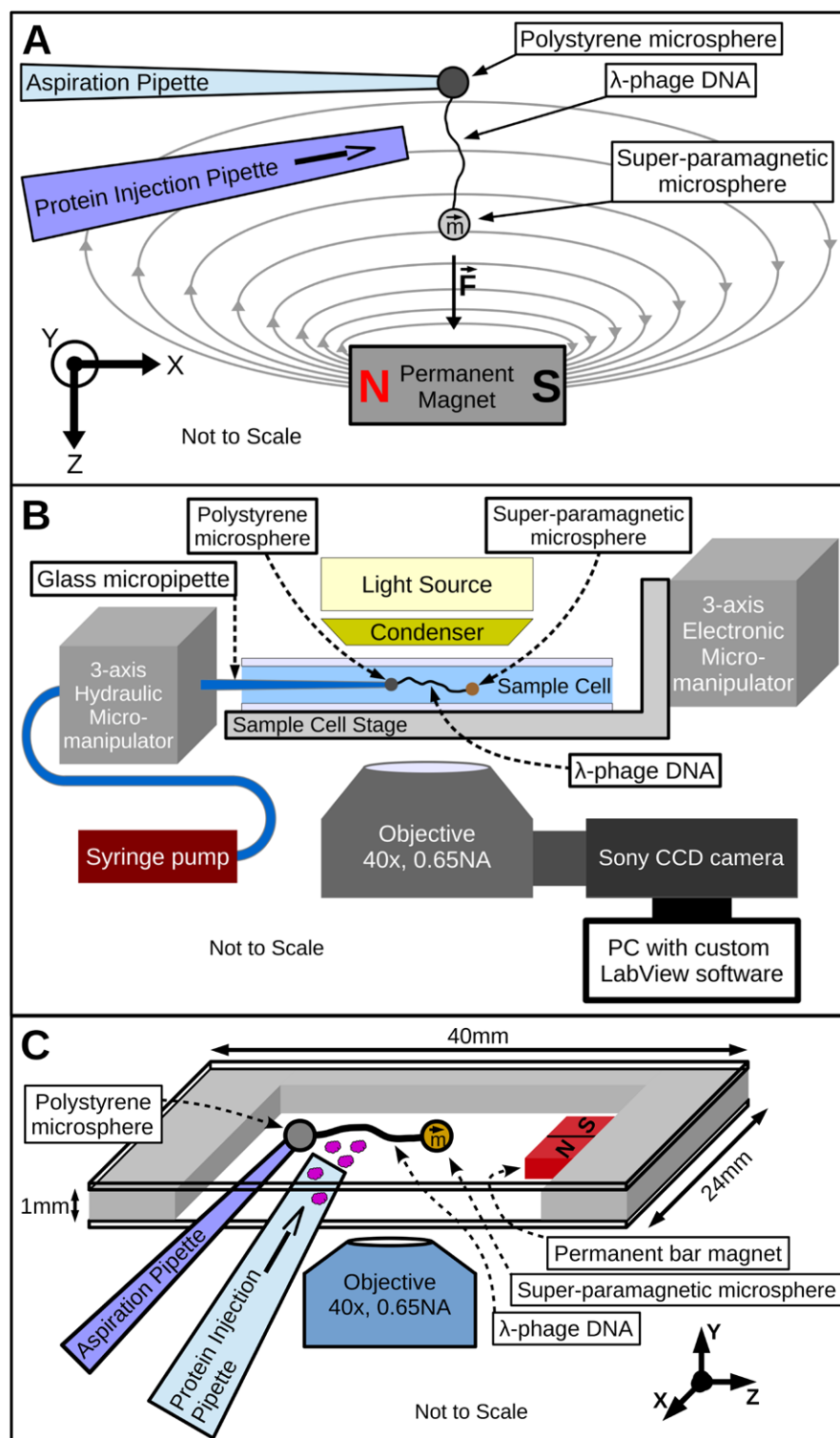


**Figure 1. Principle of horizontal magnetic tweezers.** (A) The tweezers use a glass micropipette (~1.5–2.5  $\mu\text{m}$  opening) to aspirate and manipulate a non-magnetic microsphere with a DNA tether. The other end of the tether has a superparamagnetic microparticle attached to it. Forces ranging from 0.1 pN to 20 pN (and higher) can be achieved by adjusting the DNA–magnet distance from 2000  $\mu\text{m}$  to 300  $\mu\text{m}$ . We use a bar magnet (1 mm  $\times$  2 mm  $\times$  4 mm) and define the origin at the center of the inward facing 4 mm  $\times$  1 mm magnet wall. The long axis (4 mm) of the magnet is positioned parallel to the aspiration micropipette. The plane of the paper is the plane of focus in this figure. (B) A block diagram showing the layout of the system. See Supplementary Figure S21 for an annotated photo of the assembled system showing most of the system components. (C) The design of the sample cell (cell for short) is shown. Its construction is described in the text. From the open side, we can introduce the aspiration pipette to capture bead–DNA pairs. Independent three-axis micromanipulators (not shown) are used to position the pipette and the cell above the objective. The pipette and the sample cell move independently over the 40  $\times$ , 0.65 NA microscope objective (not drawn to scale).

cently manipulate the aspiration and protein microspray pipettes (both pipettes are fixed relative to each other); (iii) by placing the pipette micromanipulator on a rail system rigidly fixed to the microscope to increase stability; and (iv) by floating the stage on a separate motorized micromanipulator that enables ease of use and adjustment of the separation between the superparamagnetic particle and the magnet. As a result, forces in the 0.01–20 pN range can be exerted and adjusted with minimal perturbation to protein-bound DNA tethers, while high precision measurements—for forces, 0.01 pN, and for extensions, <10 nm—are achievable. Our design minimizes the need for costly and complex instrumentation by using differential measurements instead of active drift compensation for hour-long experiments; however, a limitation is that DNA topology cannot be manipulated in a straightforward way.

## Materials and methods

### Magnetic tweezers

DNA end-functionalization, bead prep, DNA-bead tethering, WIF-B cell culture, histone purification, and pipette pulling and polishing protocols are described in sections 1–6 in the Supplementary Material. Section 7 of the Supplementary Material and Supplementary Figure S1 describe specialized components. This is followed by Section 8 describing the tweezers, and Supplementary Figure S2, which displays most of the major components assembled together. This should be used in conjunction with Figure 1 to visualize the general layout of the instrument. The physical dimensions of custom-made components and fixtures are also described in the relevant sections. Experimental procedures for DNA extension and histone–DNA experiments are discussed below. Data analysis techniques are explained in sections 11–14 of the Supplementary Material. Sample cell preparation and other details are discussed here and in the figure captions.

Figure 1A shows the basic principle of our tweezers, and Figure 1B shows the instrument set-up. The rectangular sample cell (henceforth referred to as the “cell”) is closed on five sides. Cells are constructed using 2 #1 coverslips (Fisher Scientific, Pittsburgh, PA), cut glass slides, and a 4 mm × 2 mm × 1 mm neodymium bar magnet (Indigo Instruments, Waterloo, Ontario, Canada). The coverslips form the floor and ceiling, and the cut sections of

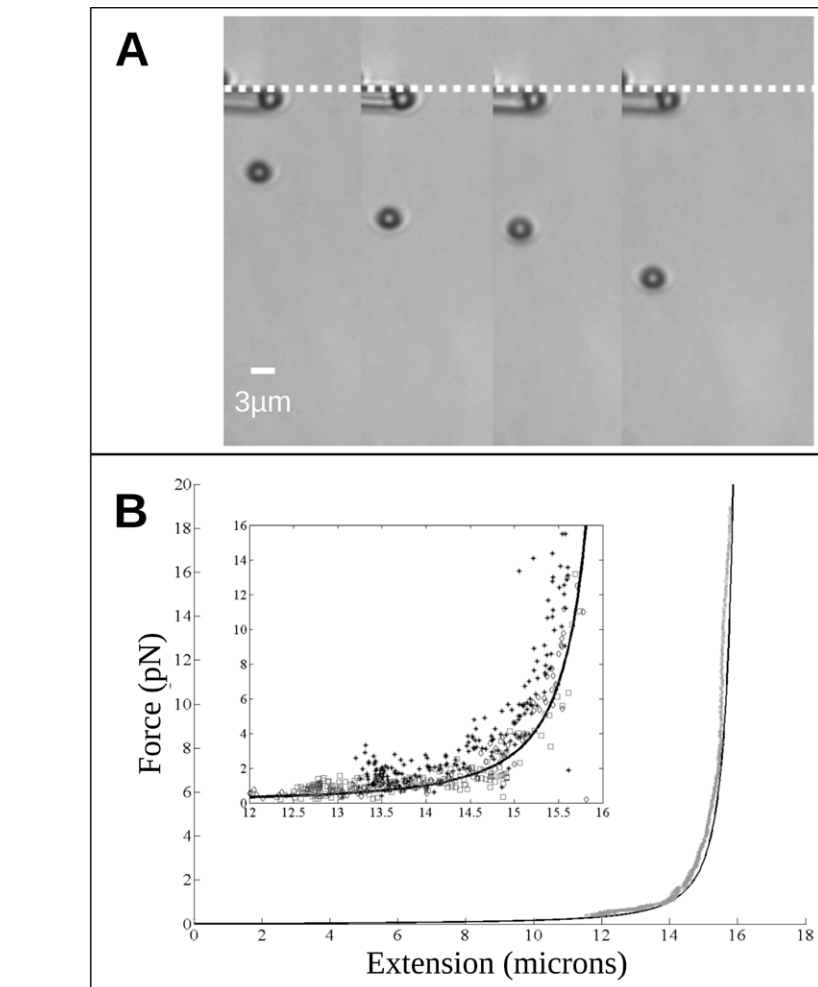


**Figure 2. Results of DNA pulling experiments.** (A) Screen shot from a DNA extension experiment. From left to right, the first snapshot shows a single DNA molecule subject to a force of ~0.5 pN at a distance of 2000  $\mu\text{m}$  from the magnet. The next image in the series shows  $\lambda$  DNA reaching toward its full 16.4  $\mu\text{m}$  extension at a force of 5 pN at a distance of ~1200  $\mu\text{m}$ . In the third panel, DNA is fully extended at a force of 20 pN at a distance of ~550  $\mu\text{m}$ . The final image shows DNA overextending in response to a force of 65 pN at a distance of 380  $\mu\text{m}$ . The dotted line corresponds to the location of the pipette throughout the experiment. This emphasizes that there is no drift throughout the entire hour-long experiment. The scale bar is 3  $\mu\text{m}$ . The magnet is far outside the available field of view and is located at the bottom of the figure. The loading rate was 0.008 pN/s. (B) Results from several DNA force-extension experiments on  $\lambda$  DNA in our horizontal magnetic tweezers. By positioning the magnet >2000  $\mu\text{m}$  from the bead–DNA constructs, we can apply low forces of 0.5–5 pN and work within DNA’s entropic response regime. By bringing the magnet closer (<1200  $\mu\text{m}$ ), higher forces (5–20 pN) can be achieved, and the DNA’s elastic regime can be studied. The solid line represents the wormlike chain theoretical model for DNA response to force, which is overlaid on data from a typical force-extension experiment from 0.5 pN to 20 pN with the magnet–DNA distance changing at 1.6  $\mu\text{m}/\text{s}$ . The inset shows a zoom-in of three separate force-extension experiments represented by the stars, diamonds, and squares at the transition from DNA’s entropic response to DNA’s elastic response.

the regular microscope slides form three of the four walls of the cell. The cut glass and the bar magnet are both glued to the bottom coverslip with clear RTV silicone sealant (DAP, Baltimore, MD). Placement of the roof coverslip results in a 1 mm × 30 mm rectangular opening designed to allow the horizontal insertion and movement of aspiration and other micropipettes. The top coverslip is placed after introduction of buffer and DNA—see Section 9, “Extension Experiments” in the Supplementary Material.

The cell is mounted on an aluminum stage that has an appropriately sized opening allowing sample illumination to pass through to the objective and is secured to the stage using clear, double-sided tape (3M, St. Paul, MN). The stage itself is attached to an Eppendorf 5171 motorized three-axis micromanipulator (Eppendorf, Hauppauge, NY) with a 0.160  $\mu\text{m}$  step size and a minimum step rate of 0.320  $\mu\text{m}/\text{s}$ . In order to make fine adjustments of the aspiration pipette over the objective, the pipette is clamped into the

arm of a hydraulic, three-axis micromanipulator (MX630L S3432; Siskiyou Corporation, Grants Pass, OR). A specially designed clip allows us to rigidly attach a protein-loaded micropipette at a fixed angle relative to the aspiration micropipette; the stage, adapter, and other specialized parts are described in the Supplementary Material.

Micromanipulators are built around a Nikon Diaphot TMD inverted light microscope (Nikon, Tokyo, Japan) with a 40×, 0.65 NA, bright-field objective (Leitz—now Leica, Wetzlar, Germany). The motorized micromanipulator is mounted on the microscope's side bench and is positioned to allow easy movement of the stage above the objective. The hydraulic manipulator is mounted on a carriage designed to bridge a rail system (Thomson Linear, Radford, VA); this allows it to easily move horizontally into the cell and out of the way when not needed or when loading pipettes.

The imaging sensor sampling rate has to be selected appropriately to allow enough time between samples for thermal averaging to take place while staying above the Nyquist limit—see References 24, 30, and 31 for the sampling rate's dependence on force and other details. In our case, videos are recorded by Labview using a Sony XCD-U100 CCD camera (Sony, Tokyo, Japan) with frame rate adjustable to 30 Hz. A zoom lens (Edmund Optics, Barrington, NJ) is inserted between the objective and the camera. Sensors with higher frame rates can also be placed in the optical path without difficulty. Data from experiments are stored on an external hard drive and analyzed on a Windows PC.

## Results and discussion

Figure 2A consists of snapshots from a force-extension experiment on a single DNA molecule showing the polymer's response to four different distance-dependent forces that act in the plane of the figure. The figure caption presents details of the experiment, and these are further discussed in the Supplementary Material. Note that a very high force of 65 pN is generated, resulting in DNA overextension (32, 33).

Figure 2B presents the results of typical force-extension experiments plotted against the modified wormlike chain model of DNA (34):

$$\frac{f_z b}{k_B T} = \frac{1}{4} \left( 1 - \frac{\langle z \rangle}{L_0} + \frac{f_z}{K_0} \right)^{-2} - \frac{1}{4} + \frac{\langle z \rangle}{L_0} - \frac{f_z}{K_0} \quad [\text{Eq. 1}].$$

Here,  $f_z$  is the applied force,  $k_B$  is Boltzmann's constant,  $T$  is the absolute temperature of  $\sim 297^\circ\text{K}$ ,  $b$  is the persistence length of 50 nm,  $L_0$  is the contour length of 16.4  $\mu\text{m}$ ,  $K_0$  is the elastic modulus of DNA,  $\sim 1000$  pN, and  $z$  is DNA's observed end-to-end extension. Our results recapitulate DNA's mechanical response in the 0.1–10 pN range (1). These data were obtained over 45 min; however experiments can last several hours. We find that the bead aspiration, buffer volume, and other experimental conditions can be stably maintained for this duration. The inset to Figure 2B shows the transition from DNA's entropy-dominated response to the Hookean elastic response; the stars and squares are from experiments performed at 0.320  $\mu\text{m/s}$ , while the diamonds are data from an experiment performed at 1.6  $\mu\text{m/s}$ . Overall, we see excellent agreement between the force-extension data and the worm-like-chain model across the range of forces for which the model is valid. The steps involved in these experiments are described in Section 9 of the Supplementary Materials.

Micromechanical experiments designed to study protein dissociation as a function of force require a method for adjusting the tension on protein-loaded DNA tethers. For this, the force must be changed slowly enough to leave the protein–DNA complex in equilibrium. A prerequisite for this is to be able to adjust tension on protein-free DNA while ensuring equilibrium. To test for the reversibility of force loads, we repeatedly extended and contracted a DNA molecule with no bound proteins. As Figure 3A shows, there is minimal hysteresis, indicating that forces can be adjusted while leaving DNA tethers in equilibrium. From these data, we extrapolate to the case of tethers with bound proteins. An extrapolation is necessary since we used histones, which unbind irreversibly beyond a certain force, implying that maintenance of binding–unbinding equilibrium as a function of force loading rates could not be tested directly. However, when we performed experiments with histones, we found that the measured critical force and other quantities agreed well with bulk experiments (where available) or theoretical estimates premised on the presence of equilibrium. Thus, we conclude that the loading rates achievable in our instrument minimally disturb bound proteins.

Force measurements obtained from our fluctuation-dissipation method were verified as follows. Using micropipettes with a 15–20  $\mu\text{m}$  opening, we released 2.8  $\mu\text{m}$

magnetic beads 300  $\mu\text{m}$  from the magnet and halfway between the floor and the roof of the cell, and then at distances from the magnet increasing in 100  $\mu\text{m}$  increments up to 2500  $\mu\text{m}$ . The buffers used were a low viscosity, 1.5 centi-Poise (cP), 25% w/v  $\text{CaCl}_2$  solution and a high viscosity, 7 cP 55% w/v glycerine (glycerol) solution (11). Magnetic particles (bead density  $\sim 1.22$   $\text{g/cm}^3$ ) are neutrally buoyant in the  $\text{CaCl}_2$  solution, while glycerine retards sedimentation. The beads quickly reached terminal velocity. The spatial rate of change of the component of the magnetic field pointing toward the magnet does not vary too greatly over a distance of 20–30  $\mu\text{m}$ , as estimated by the constancy of force over 20–30  $\mu\text{m}$  changes in distance between tethered beads and the magnet as close as 300  $\mu\text{m}$  from the magnet, which is also the approximate  $z$ -field of view (the force is defined to be in the direction of the  $z$ -axis); therefore we use the terminal velocity in Stokes' drag law (35) to evaluate the force at that location,

$$f_z = 3\pi\eta v_z d \quad [\text{Eq. 2}].$$

Here,  $\eta$  is the viscosity of the medium,  $v_z$  is the velocity in the direction of the force, and  $d$  is the bead diameter (2.8  $\mu\text{m}$ ). Because the velocity of the beads is  $\sim 10$   $\mu\text{m/s}$  and, thus, the Reynolds number is small, use of Stokes' drag law is valid. Furthermore, the effect of the vertical bounding surfaces is negligible because particle trajectories are confined to a plane well separated from them. The velocities were calculated using a custom particle tracking software described in the Supplementary Material. The buffer viscosities were measured using a Thermo Haake RheoStress 600 viscometer (Thermo Scientific, Pittsburgh, PA).

Figure 3B shows the results of these calibration experiments. The three dashed curves and one thick solid curve each represent a calibration experiment, while the thin solid curve represents the average of force measured in several DNA force-extension experiments using the fluctuation-dissipation theorem. The data correspond well with the  $\sim 1/z^4$  nature of the force produced by a dipole magnetic field that is expected along the perpendicular bisector of a bar magnet (36). The force calculated using the fluctuation-dissipation theorem agrees, within 2%–3% error, with our Stokes' drag law calculation of the force. The forces in the thin solid curve were obtained from experi-

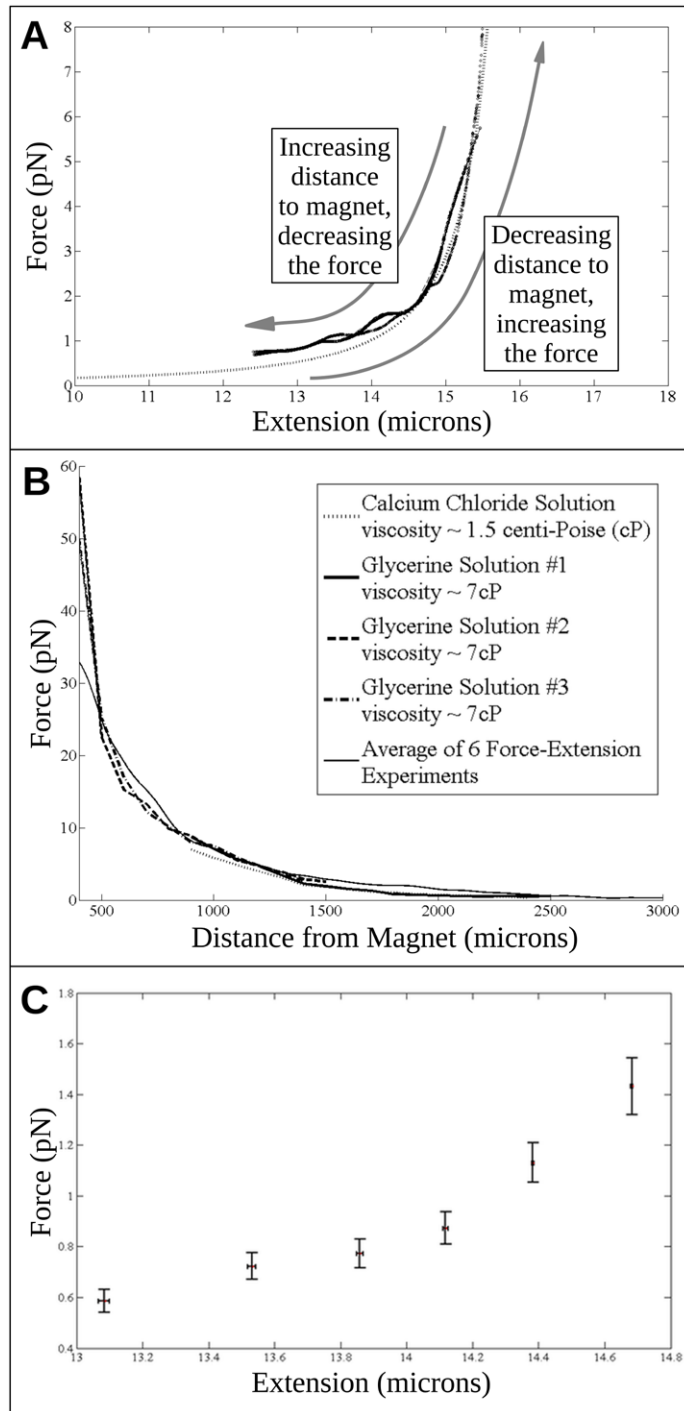


**Figure 3. Testing for hysteresis, force calibration, and precision.** (A) Stepping forces from low (<0.1 pN) to high (>50 pN) and back results in minimal hysteresis. For the data reported here, superparamagnetic particle-magnet distance was adjusted at 0.320  $\mu\text{m/s}$ . From this and the preceding figure, we see that the loading rate is low enough to nearly match the wormlike chain model (dotted line). The x-axis starts at 10  $\mu\text{m}$ . (B) Forces measured using the fluctuation-dissipation theorem compared with measurements from Stokes' drag law-based calibration experiments. Untethered superparamagnetic beads were introduced at various distances from the magnet and allowed to reach terminal velocity, which was measured using video data analysis. Stokes' drag law was used to calculate the drag force on the beads, allowing us to measure the magnetic force on the magnetic microspheres as a function of distance from the magnet. The thin solid line shows the average of six force-extension experiments as calculated from the Brownian fluctuation method. The dashed line and the dash-dotted line are the results of 2 glycerine solution experiments, which covered the range of 400 (~55 pN) to 1500  $\mu\text{m}$  (~2 pN) from the magnet. The thick solid line, another glycerine solution experiment, and the dotted line, a calcium-chloride experiment, both covered 2500  $\mu\text{m}$  (~0.5 pN) to 900  $\mu\text{m}$  (~8 pN) and overlap in the figure. (C) Data used to characterize the precision of extension and force measurements of the tweezers device. Extension and force data are subject to thermal fluctuations, which set the fundamental limit on precision. Additional noise components include localization error from video-microscopy-based centroid detection and other non-thermal (instrumental) noise sources. To quantify the precision, we performed 9 replications of an experiment in which a DNA molecule was held at specific distances from the magnet for 5 min at each location while recording force and extension data. At 2000  $\mu\text{m}$  from the magnet, the mean DNA extension was 13.08  $\mu\text{m}$  with a standard error of the mean (SEM) of 0.030  $\mu\text{m}$ , while the mean force was 0.59 pN with SEM = 0.050 pN; at 1750  $\mu\text{m}$  from the magnet, the mean extension was 13.53  $\mu\text{m}$  with SEM = 0.024  $\mu\text{m}$ , while the mean force was 0.72 pN with SEM = 0.05 pN; at 1500  $\mu\text{m}$ , a mean extension of 13.86  $\mu\text{m}$  was observed with SEM = 0.020  $\mu\text{m}$ , while the mean force was 0.77 pN with SEM = 0.060 pN; at 1250  $\mu\text{m}$ , a mean extension of 14.12  $\mu\text{m}$  was recorded with SEM = 0.017  $\mu\text{m}$ , and the mean force was calculated as 0.87 pN with SEM = 0.0638 pN; at 1000  $\mu\text{m}$ , a mean extension of 14.38  $\mu\text{m}$  was recorded with SEM = 0.0078  $\mu\text{m}$ , while a mean force of 1.13 pN was determined with SEM = 0.080 pN; and at 900  $\mu\text{m}$ , a mean extension of 14.68  $\mu\text{m}$  was found with a SEM of 0.0065  $\mu\text{m}$ , while the mean force was determined to be 1.43 pN with a SEM of 0.10 pN. These results suggest that in the range at which typical DNA-protein experiments occur (<10 pN), force precision is on the order of ~0.05 pN, and extension precision is ~10 nm (and less than 10 nm for forces >1 pN).

ments done at a combination of loading rates of 0.320  $\mu\text{m/s}$  or 1.6  $\mu\text{m/s}$ . There is good agreement between force extension measurements and the calibration experiments up to ~35 pN. Beyond ~35 pN or for distances to the magnet closer than 350  $\mu\text{m}$ , the calibration technique breaks down because the magnetic microspheres do not reach terminal velocity within the objective's field of view.

In order to determine the precision (i.e., the reproducibility) with which we

can measure changes in tether extension and to determine the smallest forces we can reliably control, we carried out force and extension measurements on identical tethers at fixed distances from the magnet (Figure 3C). We found that forces of ~0.05 pN and extension changes of ~10 nm (and less) can be reproducibly measured from our data, and we note that these are comparable to the force and extension resolution limits of ~0.05 pN and ~5 nm (see Supplementary Material Appendix

for detailed calculations). This makes our instrument well-suited for studying the binding and unbinding events of many DNA-compacting proteins.

We investigated the feasibility of protein-DNA experiments using our tweezers by testing whether individual core histone octamer unbinding transitions could be detected at low forces of ~2 pN that had not been reported before. The steps involved in these experiments are described in the Supplementary Material

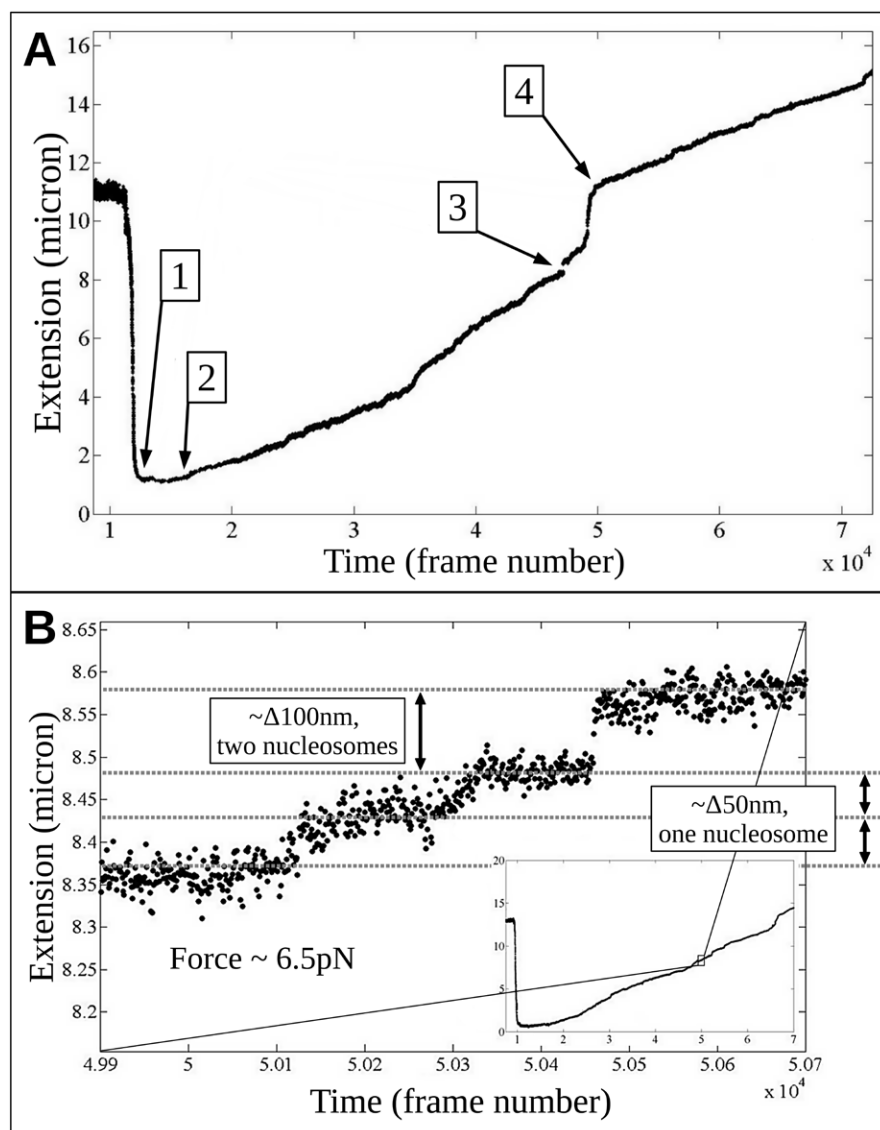


**Figure 4. Histone-mediated DNA compaction.** (A) The course of an entire histone–DNA complex reconstitution–disruption experiment is shown. The horizontal axis is the frame number, which corresponds to the time, while the vertical axis is the molecule’s end-to-end extension in microns. The experiment was performed by first extending a single  $\lambda$  DNA molecule at  $\sim 1$  pN. Then, core histone proteins were sprayed onto the molecule. This is signaled by the rapid drop in the extension of the molecule. After histones were bound, the force was slowly increased. Eventually, the molecule’s starting extension of  $\sim 12 \mu\text{m}$  was recovered. At arrow 1, proteins are stably bound to a single DNA tether at a low force. The force is increased very slowly ( $\sim 0.008$  pN/s) beginning at arrow 2, and the proteins begin to dissociate from the DNA molecule. Arrow 3 indicates a region of higher force (12.5 pN) with an increased rate of protein dissociation. The DNA tether finally reaches its starting extension at a sufficiently high force to eject nearly all proteins at arrow 4. (B) This shows typical higher-resolution extension data selected from the boxed region of the inset  $\sim 0.5$  h after tether compaction. These data correspond to a 1 min window within the experiment when the force was  $\sim 6.5$  pN. The quantized  $\sim 50$  nm changes in extension that are seen are the rupturing of the individual nucleosome-like complexes, showing that we can detect their dissolution very near the theoretically predicted force value. The entire experiment lasted approximately 1 h 45 min. After a tethered DNA is found and captured, we bring the magnet within 1000  $\mu\text{m}$  of the molecule to subject it to a force of  $\sim 9$  pN. The observed extension of the DNA allows us to check that the tether is indeed a single molecule of DNA. Then we step the magnet away from the DNA at a rate of 1.6  $\mu\text{m/s}$  so that the distance between the bead and the magnet is 2 mm, corresponding to a force of  $\sim 0.8$  pN. Next, using a pre-loaded, pre-positioned protein spray pipette aimed at the tip of the aspiration pipette, we introduce the histones by spraying them onto the extended DNA. We can detect the protein solution flow past the captured pair since the DNA is deflected to the right from its equilibrium position. We then observe a rapid  $\sim 1$  min contraction of the tether, indicating binding of histones to the DNA. After completion of the contraction step, we quasi-statically move through the force range starting from forces below the theoretically predicted rupture force of  $\sim 2.5$  pN to somewhat higher forces while monitoring the DNA extension (off-line) for the signatures of histone complex unbinding.

under “Histone-DNA Experiments.” As shown in the data presented in Figure 4, force-induced unbinding events could be detected at low forces. Histone proteins H2A, H2B, H3, and H4 were introduced into the sample cell by microinjection from the protein-loaded micropipette and allowed to interact with a  $\lambda$ -DNA molecule that had been extended by applying a small force of  $\sim 1$  pN. This force was enough to extend the tether but not hinder the spontaneous assembly of histones onto the DNA as evidenced by rapid tether compaction. We then subjected the histone-complexed DNA tether to higher forces to begin dissociating histone complexes. Force-induced ruptures were detected by discrete jumps in the tether extension of  $\sim 50$  nm or integer multiples of this unit. This continued until the DNA recovered its starting extension.

The time course of the DNA’s extension during a typical experiment is shown in Figure 4A: pre-spray with an initial extension of  $\sim 11 \mu\text{m}$ , spray followed by contraction to about  $\sim 1.5 \mu\text{m}$ , and re-extension to  $\sim 11+ \mu\text{m}$ . After introduction of proteins, we observe rapid contraction usually in 1 min with either full contraction or almost all of the tether extension used up. The association of histones with DNA is so rapid that we do not detect individual binding steps. Once the histones are bound, we allow the condensed DNA to remain at the low-force, protein injection position for 1 min. Then we begin to slowly ( $\sim 0.320 \mu\text{m/s}$ ) decrease the distance between the magnet and the bead, or equivalently increase the force at a loading rate of  $\sim 0.008$  pN/s. At this low loading rate, the force is essentially constant over a period of 30 s. After contraction, the first arrow in Figure 4A highlights a plateau in the extension trace indicating a region of force where the histone–DNA complexes are stable even in the presence of an applied force. The second arrow indicates a region beginning a slow, steady rate of dissociation events at forces between 2.5 and 12.5 pN. The third arrow indicates the beginning of a region of high force,  $>12.5$  pN, where one can observe a rapid unbinding of histone complexes as the molecule eventually reaches its starting extension at the fourth arrow. Figure 4B highlights a region, marked by the rectangle in the inset, of moderate force ( $\sim 6.5$  pN) where a steady rate of individual histone–DNA complex unbinding events can be observed. The identified steps

correspond to the rupture of 1 (50 nm) or 2 (100 nm) core octamer–DNA complexes. These unbinding events occurred approximately 1 h into a 2 h experiment and about 20 min after protein introduction.

A number of studies have examined the micromechanical behavior of single DNA tethers loaded with histone octameric core complexes (for recent reviews see References 37 and 38). A detailed comparison between our data and those in the literature is forthcoming and is not straightforward, since results depend strongly on loading rates (37) and other factors. Briefly, the critical force measured using our methodology is consistent with theoretical estimates (39) and is in the same range as other magnetic tweezers studies (37).

## Author contributions

C.P.M. and C.T. carried out the experiments and data analysis. J.Z. carried out part of the data analysis. C.P.M., C.T., P.M., and A.S. designed the instrument. I.L.P., P.T., and A.S. designed and supervised the experiments and assisted with the data analysis. C.P.M., C.T., I.L.P., P.T., and A.S. wrote the manuscript.

## Acknowledgments

We gratefully acknowledge the assistance of the following individuals: Dunja Skoko, C.L. Chou, Eric Fischer, Robert Mohr, Paul Branch, Benjamin Buckeye, Helen DeCelles-Zwerneman, Jonathan Luke, Roberto Fabian, Ryan Vilbig, Anneliese Striz, and Mark Knepper. A. Sarkar would like to acknowledge funding from Vitreous State Laboratory and The Catholic University of America. P. Tuma wishes to thank the NIH for partially funding this research through R01 AA17626. This paper is subject to the NIH public access policy.

## Competing interests

The authors declare no competing interests.

## References

- Smith, S.B., L. Finzi, and C. Bustamante. 1992. Direct mechanical measurements of the elasticity of single DNA molecules by using magnetic beads. *Science* 258:1122–1126.
- Strick, T.R., J.-F. Allemand, D. Bensimon, A. Bensimon, and V. Croquette. 1996. The elasticity of a single supercoiled DNA molecule. *Science* 271:1835–1837.
- Strick, T., J. Allemand, V. Croquette, and D. Bensimon. 2000. Twisting and stretching single DNA molecules. *Prog. Biophys. Mol. Biol.* 74:115–140.
- Gosse, C. and V. Croquette. 2002. Magnetic tweezers: micromanipulation and force measurement at the molecular level. *Biophys. J.* 82:3314–3329.
- Neuman, K.C. and A. Nagy. 2008. Single-molecule force spectroscopy: optical tweezers, magnetic tweezers and atomic force microscopy. *Nat. Methods* 5:491–505.
- Seol, Y. and K.C. Neuman. 2011. Magnetic tweezers for single-molecule manipulation. *Methods Mol. Biol.* 783:265–293.
- Lionnet, T., J.F. Allemand, A. Revyakin, T.R. Strick, O.A. Saleh, D. Bensimon, and V. Croquette. 2012. Magnetic trap construction. *Cold Spring Harb. Protoc.* 2012:133–128.
- Lipfert, J., M. Lee, O. Ordu, J. Kerssemakers, and N.H. Dekker. 2014. Magnetic Tweezers for the Measurement of Twist and Torque. *J. Vis. Exp.* 87:e51503.
- Strick, T.R., J.F. Allemand, D. Bensimon, and V. Croquette. 1998. Behavior of supercoiled DNA. *Biophys. J.* 74:2016–2028.
- Kollmannsberger, P. and B. Fabry. 2007. High-force magnetic tweezers with force feedback for biological applications. *Rev. Sci. Instrum.* 78:114301.
- Haber, C. and D. Wirtz. 2000. Magnetic tweezers for DNA micromanipulation. *Rev. Sci. Instrum.* 71:4561–4570.
- Zacchia, N.A. and M.T. Valentine. 2015. Design and optimization of arrays of neodymium iron boron-based magnets for magnetic tweezers applications. *Rev. Sci. Instrum.* 86:053704.
- Mosconi, F., J.F. Allemand, and V. Croquette. 2011. Soft magnetic tweezers: a proof of principle. *Rev. Sci. Instrum.* 82:034302–034314.
- Janssen, X.J.A., J. Lipfert, T. Jager, R. Daudey, J. Beekman, and N.H. Dekker. 2012. Electromagnetic Torque Tweezers: A Versatile Approach for the Measurement of Single-Molecule Twist and Torque. *Nano Lett.* 12:3634–3639.
- Lipfert, J., M. Wiggins, J.W. Kerssemakers, F. Pedaci, and N.H. Dekker. 2011. Freely orbiting magnetic tweezers to directly monitor changes in the twist of nucleic acids. *Nat Commun.* 2:439.
- Yang, Y., J. Lin, R. Meschewski, E. Watson, and M.T. Valentine. 2011. Portable magnetic tweezers device enables visualization of the three-dimensional microscale deformation of soft biological materials. *Biotechniques* 51:29–34.
- Kim, K. and O.A. Saleh. 2009. A high-resolution magnetic tweezer for single-molecule measurements. *Nucleic Acids Res.* 37:e136.
- Trepac, X., M. Grabulosa, L. Buscemi, F. Rico, B. Fabry, J.J. Fredberg, and R. Farré. 2003. Oscillatory magnetic tweezers based on ferromagnetic beads and simple coaxial coils. *Rev. Sci. Instrum.* 74:4012–4020.
- Chen, L., A. Offenhäusser, and H.J. Krause. 2015. Magnetic tweezers with high permeability electromagnets for fast actuation of magnetic beads. *Rev. Sci. Instrum.* 86:044701.
- Lansdorp, B.M., S.J. Tabrizi, A. Dittmore, and O.A. Saleh. 2013. A high-speed magnetic tweezer beyond 10,000 frames per second. *Rev. Sci. Instrum.* 84:044301.
- Lin, J., F. Persson, J. Fritzsche, J.O. Tegenfeldt, and A.O. Saleh. 2012. Bandpass filtering of DNA elastic modes using confinement and tension. *Biophys. J.* 102:96–100.
- You, H., J. Wu, F. Shao, and J. Yan. 2015. Stability and kinetics of c-MYC promoter G-quadruplexes studied by single-molecule manipulation. *J. Am. Chem. Soc.* 137:2424–2427.
- Klaue, D. and R. Seidel. 2009. Torsional Stiffness of Single Superparamagnetic Microspheres in an External Magnetic Field. *Phys. Rev. Lett.* 102:028302.
- Huhle, A., D. Klaue, H. Brutzer, P. Daldrop, S. Joo, O. Otto, U.F. Keyser, and R. Seidel. 2015. Camera-based three-dimensional real-time particle tracking at kHz rates and Ångström accuracy. *Nat Commun.* 6:5885.
- Chen, H., H. Fu, X. Zhu, P. Cong, F. Nakamura, and J. Yan. 2011. Improved high-force magnetic tweezers for stretching and refolding of proteins and short DNA. *Biophys. J.* 100:517–523.
- Yan, J., D. Skoko, and J.F. Marko. 2004. Near-field-magnetic-tweezer manipulation of single DNA molecules. *Phys. Rev. E Stat. Nonlin. Soft Matter Phys.* 70:011905–011905-5.
- Danilowicz, C., C.H. Lee, K. Kim, K. Hatch, V.W. Coljee, N. Kleckner, and M. Prentiss. 2009. Single molecule detection of direct, homologous, DNA/DNA pairing. *Proc. Natl. Acad. Sci. USA* 106:19824–19829.
- Sun, B., K. Wei, B. Zhang, X. Zhang, S. Dou, M. Li, and X. Xi. 2008. Impediment of *E. coli* UvrD by DNA-destabilizing force reveals a strained-inchworm mechanism of DNA unwinding. *EMBO J.* 27:3279–3287.
- Schwarz, F.W., J. Tóth, K. van Aelst, G. Cui, S. Clausing, M.D. Szczelkun, and R. Seidel. 2013. The helicase-like domains of type III restriction enzymes trigger long-range diffusion along DNA. *Science* 340:353–356.
- Moffitt, J.R., Y.R. Chemla, S.B. Smith, and C. Bustamante. 2008. Recent advances in optical tweezers. *Annu. Rev. Biochem.* 77:205–228.
- Lansdorp, B.M. and O.A. Saleh. 2012. Power spectrum and Allan variance methods for calibrating single-molecule video-tracking instruments. *Rev. Sci. Instrum.* 83:025115.
- Smith, S.B., Y. Cui, and C. Bustamante. 1996. Overstretching B-DNA: the elastic response of individual double-stranded and single-stranded DNA molecules. *Science* 271:795–799.
- Cluzel, P., A. Lebrun, C. Heller, R. Lavery, J.L. Viovy, D. Chatenay, and D.F. Caron. 1996. DNA: an extensible molecule. *Science* 271:792–794.
- Marko, J.F. and E.D. Siggia. 1995. Stretching DNA. *Macromolecules* 28:8759–8770.
- Brodkey, R.S. 1967. *The Phenomena of Fluid Motions*. Addison-Wesley, Reading, MA.
- Jackson, J.D. 1999. *Classical Electrodynamics*, Third Edition. Wiley, New York, NY.
- Bednar, J. and S. Dimitrov. 2011. Chromatin under mechanical stress: from single 30 nm fibers to single nucleosomes. *FEBS J.* 278:2231–2243.
- Lavelle, C., J.M. Victor, and J. Zlatanova. 2010. Chromatin fiber dynamics under tension and torsion. *Int. J. Mol. Sci.* 11:1557–1579.
- Marko, J.F. and E.D. Siggia. 1997. Driving proteins off DNA using applied tension. *Biophys. J.* 73:2173–2178.

Received 27 February 2014; accepted 08 September 2015.

Address correspondence to Abhijit Sarkar, Department of Physics, The Catholic University of America, 620 Michigan Avenue NE, Washington DC, 20064. E-mail: sarkar@cua.edu

To purchase reprints of this article, contact: [biotechniques@fosterprinting.com](mailto:biotechniques@fosterprinting.com)